J Electr Eng Technol Vol. 8, No. 3: 507-515, 2013
http://dx.doi.org/10.5370/JEET.2013.8.3.507

ISSN(Print) 1975-0102
ISSN(Online) 2093-7423

A 2^{nd} Order Harmonic Compensation Method for Wind Power System Using a PR Controller

Hae-Gwang Jeong*, Jong-Hyun Lee* and Kyo-Beum Lee†

Abstract – This paper proposes a compensation method for the 2^{nd}-order harmonic of single-phase grid-connected wind power generation systems. Theoretically, a single-phase grid-connected inverter system has no choice but to cause the 2^{nd}-order harmonic to DC-link voltage. The reference active current is affected by the DC-link voltage. The output current from the reference active current is distorted by the 1^{st} and 3^{rd}-order harmonic. The proposed method can compensate, conveniently, the reference active current with the 2^{nd}-order harmonic. To reduce the 2^{nd}-order ripple in the reference active current, proposed method takes a PR controller as a feed-forward compensator. PR controllers can implement selective harmonic compensation without excessive computational requirements; the use of these controllers simplifies the method. Both the simulation and experimental results agree well with the theoretical analysis.

Keywords: Single-phase, Grid-connected system, Wind power, Generation system, PR(Proportional Resonant) controller, 2^{nd} order harmonic

1. Introduction

AS the increase of energy demand, the black-out problems in the U.S. and Europe and the oil price instability are boosting the attention toward renewable energy and distributed power generation systems such as wind turbines, photovoltaic systems, fuel cells, micro gas turbines, small hydro units, and biomass units [1, 2].

Among the renewable power source technologies in power generation being vigorously developed, wind turbine technology has noticeably increased worldwide, i.e., from 7600 MW installed in 1997 to 122,000 MW at the end of 2008, and it is expected to reach 343,000 MW by 2013. This growing trend is stimulating research in the power processing field aimed at optimizing energy extraction from wind power and energy injection into the grid. Under this circumstance, the contribution of wind power generation systems is becoming more and more important [3-5].

The output power range of small sized wind turbine systems is from 5 KVA to 25 KVA. The small sized wind turbine systems are used for the residential houses or small sized business complex extending application fields. There are various advantages of the small sized wind turbines can more rapidly follow the change of the wind speed than the large-scale wind turbines system due to their smaller inertia. This feature contributes high power generation efficiency of the wind turbines in the case that the wind speed frequently changes [6, 7].

Generally, the small sized wind turbine is single-phase grid-connected system. The single-phase grid-connected wind power generation system needs the maximum power point tracking (MPPT) control technique, the current control of DC/DC converter, the DC-link voltage control, the current control of DC/AC inverter and anti-islanding protection.

In particular, the DC-link voltage in a single-phase wind power generation system has unavoidably twice component of fundamental wave. The 2^{nd}-order harmonic in the DC-link voltage influence the reference active current. The reference active current makes the output current to be distorted. As a result, the 2^{nd}-order harmonic in the DC-link voltage not only increase the THD but also decrease the total power efficiency [8, 9].

To solve the problems, the conventional method eliminates the ripple of DC-link voltage by using a band stop filter (BSF) and the calculation results of the 2^{nd}-order harmonic in DC-link voltage. Although the calculation result and the BSF are used together in series to eliminate the ripple of DC-link voltage, the calculation results of the 2^{nd}-order harmonic could be inaccurate and the transient response of the BSF is poor [9].

This paper proposes compensation method that reduces the 2^{nd}-order harmonic in not the DC-link voltage but the reference active current using a PR controller. Because the PR controller can take the 2^{nd}-order harmonic from the reference active current without mathematical calculation, the PR controller can be used as a feed-forward compensator.

A PSIM simulation and experiment results attained by using a 3-kW wind power system confirm the feasibility and effectiveness of the proposed method.

† Corresponding Author: Department of Electrical and Computer Engineering, Ajou University, Suwon, Korea. (kyl@ajou.ac.kr)
* Department of Electrical and Computer Engineering, Ajou University, Suwon, Korea. (lite88@ajou.ac.kr; yohann53@naver.com)
Received: July 23, 2012; Accepted: November 12, 2012

2. Wind Power Generation System

2.1 Single-Phase grid-connected wind power system

A single-phase grid-connected wind power system is shown in Fig. 1. This system is comprised of a blade, a generator, a rectifier, a buck-boost converter, a DC-link capacitor, and an H-bridge inverter. The mechanical torque produced from the wind is converted into electrical energy through the PMSG. The produced electrical energy is transferred to the DC-link capacitor through the rectifier and the buck-boost converter. The transferred DC-link electrical energy is supplied to the grid through the H-bridge inverter. The machine-side converter performs the torque control needed for Maximum Power Point Tracking (MPPT) [10].

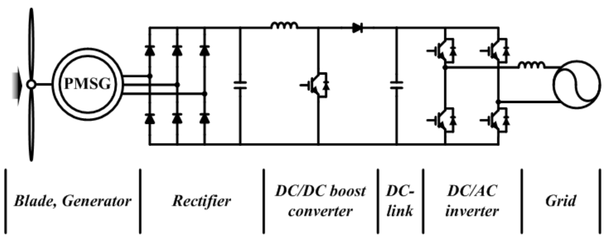

Fig. 1. Grid-connected wind power system.

2.2 Generation of the 2nd-order harmonic in the DC-link voltage

Fig. 2 shows a single-phase H-bridge DC/AC inverter system. The DC-link power from the capacitor C_{dc} is used to generate the AC grid V_{ac}. The grid voltage V_{ac} and grid current I_{ac} are defined as follows:

$$V_{ac} = V_m \cos\omega t \quad (1)$$

$$I_{ac} = I_m \cos\omega t \quad (2)$$

where $\omega=2\pi f$.

The input power P_{dc} and output AC power P_{ac} of the DC/AC inverter are calculated as:

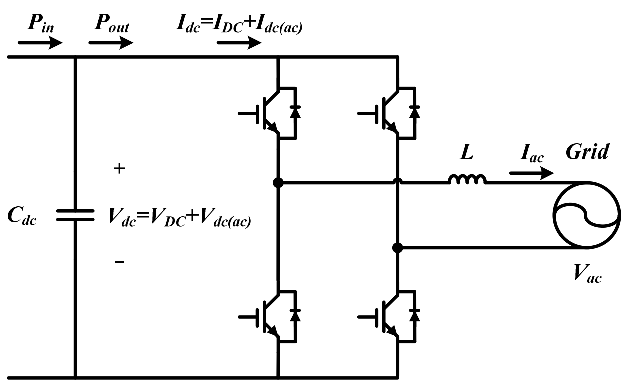

Fig. 2. Single-phase H-bridge DC/AC inverter system.

$$P_{dc} = V_{dc} I_{dc} \quad (3)$$

$$P_{ac} = V_m I_m \cos^2 \omega t = \frac{V_m I_m}{2}(1+\cos 2\omega t) \quad (4)$$

Since $P_{dc}= P_{ac}$, the DC-link current I_{dc} is derived from Equation (3) and (4). Therefore, I_{dc} consists of dc component I_{dc} and the ac component $I_{dc(ac)}$ like Equation (5).

$$I_{dc} = \frac{V_m I_m}{2V_{dc}}(1+\cos 2\omega t) = I_{DC} + I_{dc(ac)}$$

$$\text{where,}\quad I_{DC} = \frac{V_m I_m}{2V_{dc}} \quad I_{dc(ac)} = \frac{V_m I_m}{2V_{dc}}\cos 2\omega t \quad (5)$$

Thus, the DC-link voltage ripple $V_{dc(ac)}$ can be calculated by integrating the AC component $I_{dc(ac)}$ as (6) and indicating that $V_{dc(ac)}$ contains the 2nd-order harmonic with the same phase as the grid voltage V_{ac}.

$$\begin{aligned} V_{dc(ac)} &= \frac{1}{C_{dc}}\int I_{dc(ac)}dt = \frac{V_m I_m}{2V_{dc}\cdot C_{dc}}\frac{1}{2\omega}\cdot\sin 2\omega t \\ &= \frac{V_m I_m}{4\omega C_{dc} V_{dc}}\cdot \sin 2\omega t = V_{m(ac)}\sin 2\omega t \end{aligned} \quad (6)$$

It can be seen that the V_{dc} and I_{dc} consist of DC and AC components which are mainly 2nd-order harmonic, respectively [8].

2.3 Generation of the 1st and 3rd-order harmonic in the output current

Fig. 3 shows the DC-link voltage control block diagram of the single-phase grid-connected inverter system. The inverter delivers the average power from DC-side to AC-side. In this system, the inverter system controls the DC-link voltage [11]. The DC-link voltage of the inverter system has the 2nd-order harmonic in the nature of things. This harmonic has a harmful effect on the reference active current I_{de}^*. The reference active current subjected to the influence of the 2nd-order harmonic causes the distortion into the output current. The difference between the reference DC-link voltage and actual DC-link voltage would be the input value of the voltage controller. The voltage controller generates reference active current I_{de}^* with 2nd-order harmonic. The difference between the reference currents and actual currents would be input value of the PI controller. This PI controller generates the reference voltage in the synchronous frame. These reference voltages in the synchronous frame are transformed to reference voltages in the stationary frame through frame transformation. In this process, the 2nd-order harmonic is converted into 1st and 3rd-order harmonic. These harmonic make the output current to be distorted.

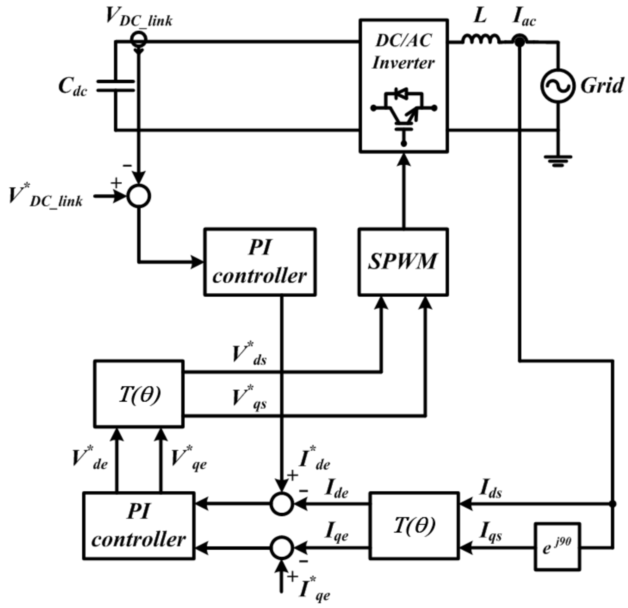

Fig. 3. Single-phase H-bridge DC/AC inverter system

The reference active current I_{de}^* and the reference reactive current I_{qe}^* frame can be expressed as follows:

$$I_{de}^* = I_{DE}^* \cos 2\omega t, \quad I_{qe}^* = 0 \tag{7}$$

In the synchronous reference frame, Equation (8) shows the reference active voltage V_{de}^* and the reference reactive voltage V_{qe}^* which are obtained from the PI controller.

$$V_{de}^* = V_{DE}^* \cos 2\omega t, \quad V_{qe}^* = V_{QE}^* \sin 2\omega t \tag{8}$$

In the stationary reference frame, equation (9) and (10) show the reference active voltage V_{ds}^* and the reference reactive voltage V_{qs}^*, respectively, which can be made by doing frame transformation.

$$\begin{aligned} V_{ds}^* &= V_{de}^* \sin \omega t - V_{qe}^* \cos \omega t \\ &= V_{DE}^* \cos 2\omega t \sin \omega t - V_{QE}^* \sin 2\omega t \cos \omega t \\ &= \left(\frac{V_{DE}^*}{2} - \frac{V_{QE}^*}{2} \right) \sin 3\omega t - \left(\frac{V_{DE}^*}{2} + \frac{V_{QE}^*}{2} \right) \sin \omega t \end{aligned} \tag{9}$$

$$\begin{aligned} V_{qs}^* &= V_{de}^* \cos \omega t + V_{qe}^* \sin \omega t \\ &= V_{DE}^* \cos 2\omega t \cos \omega t + V_{QE}^* \sin 2\omega t \sin \omega t \\ &= \left(\frac{V_{DE}^*}{2} - \frac{V_{QE}^*}{2} \right) \cos 3\omega t + \left(\frac{V_{DE}^*}{2} + \frac{V_{QE}^*}{2} \right) \cos \omega t \end{aligned} \tag{10}$$

The reference active voltage V_{ds}^* and the reference reactive voltage V_{qe}^* in the stationary reference frame are used to SPWM. Because these values have 1st and 3rd-order harmonic, the output current is distorted by 1st and 3rd-order harmonic. As a result, the 2nd-order harmonic of the DC-link voltage makes the output current to be distorted.

3. Conventional Method of 2nd-order Harmonic Compensation

3.1 Calculation of the ripple component

When the constant input power is flowed into the DC-link capacitor, the DC-link voltage has the 2nd-order harmonic because the grid-side instantaneous power contains the ripple component. Thus, the 2nd-order harmonic can be calculated and compensate the DC-link voltage.

Considering the power flow of between the DC/DC converter and DC/AC inverter in Fig. 2, the instantaneous power of the DC-link is shown as follows:

$$\frac{d}{dt}\left(\frac{1}{2} C_{dc} V_{dc}^2 \right) = p_{in} - p_{out} \tag{11}$$

The mean value of output power p_{out} in the steady state is shown in Equation (12).

$$p_{out} = \frac{I_m V_m}{2} \tag{12}$$

It is possible to make Equation (13) using Equation (11) and (12).

$$p_{in} = C_{dc} V_{dc} \frac{dV_{dc}}{dt} + \frac{I_m V_m}{2} \tag{13}$$

Assuming no power loss at the DC/AC inverter, the power flow at the DC-link side can be expressed as follows:

$$p_{in} - \frac{d}{dt}\left(\frac{1}{2} C_{dc} V_{dc}^2 \right) = \frac{d}{dt}\left(\frac{1}{2} L i_{ac}^2 \right) + \frac{V_m I_m}{2} + \frac{V_m I_m}{2} \cos 2\omega t \tag{14}$$

Because the input power is same as the instantaneous mean power of grid-side, Equation (14) can be arranged by substituting $i_{ac} = I_m \cos \omega t$ as follows:

$$C_{dc} V_{dc} \frac{dV_{dc}}{dt} = \frac{\omega L I_m^2}{2} \sin 2\omega t - \frac{V_m I_m}{2} \cos 2\omega t \tag{15}$$

Because the ripple component of DC-link voltage is smaller than the reference of DC-link voltage, Equation (15) can be expressed as follows:

$$C_{dc} V_{dc}^* \frac{d\tilde{V}_{dc}}{dt} = \frac{\omega L I_m^2}{2} \sin 2\omega t - \frac{V_m I_m}{2} \cos 2\omega t \tag{16}$$

where V_{dc}^* is the reference of DC-link voltage and $\tilde{V}_{dc}$ is the ripple component of DC-link voltage. The ripple component of DC-link voltage can be obtained from Equation (16) as follows:

$$\tilde{V}_{dc} = \frac{1}{C_{dc}V_{dc}^*}\left(\frac{LI_m^2}{4}\cos 2\omega t + \frac{V_m I_m}{4\omega}\sin 2\omega t\right) \tag{17}$$

3.2 2nd-order harmonic compensation with the calculation results and band stop filter (BSF)

When the parameter values are accurate, the method of ripple component calculation has good performance to compensate the ripple. However, when the parameter values are inaccurate, the method of ripple component calculation has the poor performance. Thus, the conventional method of 2nd-order harmonic compensation successively used the band stop filter (BSF) and the calculation of ripple component to improve transient state and steady state. Fig. 4 shows the conventional ripple elimination method.

The conventional method is complicated. To calculate the ripple component, accurate parameter values should be needed as mentioned earlier. The calculations also must be performed correctly. In addition, BSF which has poor transient performance should be needed to complete the elimination of ripple component.

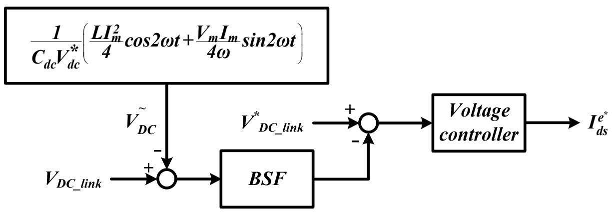

Fig. 4. Block diagram of conventional ripple elimination method.

4. Proposed Method of 2nd-order Harmonic Compensation

The 2nd-order harmonic, structurally, have no choice but to cause into the DC-link voltage of the single-phase grid-connected system. In addition, the distorted output current is owing to the reference active current. That is why, in contrast to the conventional method, the proposed method compensates not the reference of DC-link voltage but the reference active current using PR controller as a feed-forward compensator. The output current can be compensated by improving the reference active current. Because of the feature of PR controller, compensating reference active current with the PR controller does not need complicated calculation as the conventional method.

4.1 Feature of PR controller

The PR controller is used in the stationary frame. In contrast to the PI controller used in the synchronous frame, the computation sequence of the PR controller is shortened because there is no transforming frame from the stationary frame to synchronous frame as in PI controller. It is possible to replace the PI controller in the synchronous frame with the PR controller in the stationary frame. This frequency-modulating process can be mathematically expressed as:

$$G_{AC}(s) = G_{DC}(s - j\omega) + G_{DC}(s + j\omega) \tag{18}$$

where $G_{AC}(s)$ represents the equivalent stationary-frame transfer function [12]. Therefore, for the integrator of $G_{DC}(s) = K_i/(1+(s/\omega_c))$, where K_i represents the controller gain and $\omega_c << \omega$ represents the cutoff frequency, the derived AC integrators $G_{AC}(s)$ are expressed as [13, 14]:

$$\begin{aligned} G_{AC}(s) = \frac{Y(s)}{E(s)} &= \frac{2K_i(\omega_c s + \omega_c^2)}{s^2 + 2\omega_c s + (\omega_c^2 + \omega^2)} \\ &\approx \frac{2K_i(\omega_c s + \omega_c^2)}{s^2 + \omega_c s + \omega^2} \end{aligned} \tag{19}$$

When a proportional term K_p is added to Equation (19), it represents the PR controller with an high gain at the frequency of ω (see Fig. 5) but at no other frequencies. K_p is tuned in the same way as the PI controller, which determines the dynamics of the system in terms of the bandwidth, phase, and gain margin. Although its gain is finite, it is relatively high in order to give a small steady-state error. The bandwidth can be widened by tuning ω_c appropriately. This reduces the sensitivity to the slight frequency variation that occurs in a typical grid [15].

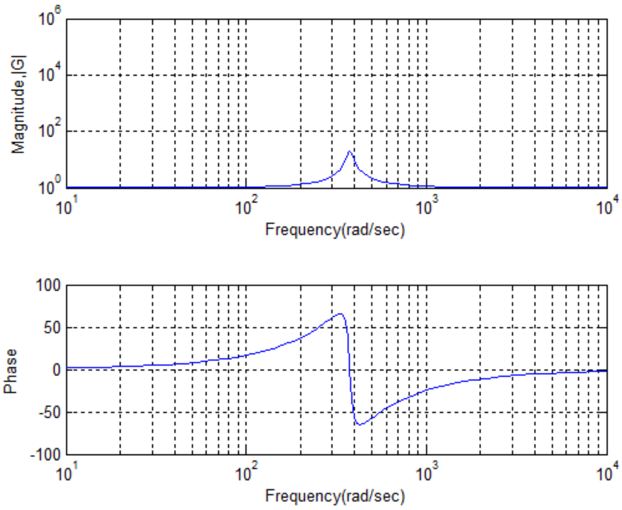

Fig. 5. Bode plots of the PR compensators; K_p=1, K_i=20, ω=377rad/s, and ω_c=10rad/s.

4.2 Compensation of 2nd-order harmonic in the reference active current using PR controller

As earlier mentioned, the PR controller is used in stationary frame, originally. However, the PR controller can be used the harmonic compensator regardless of the frame type. Thus, it is possible to compensate for the harmonic using the PR controller, which has a relatively high gain in a specific frequency band. The harmonic can be compensated selectively by adjusting the frequency of the low-order harmonic. Equation (20) is the transfer function of the 2nd-order harmonic compensator (HC) [16].

$$G_h(s) = \sum_{h=2} \frac{2K_{ih}\omega_c s}{s^2 + 2\omega_c s + (h\omega)^2} \tag{20}$$

where h is the harmonic order to compensate for, and K_{ih} represents the individual resonant gain. Resonance peak can be adjusted by controlling the K_{ih} which must be tuned relatively high (but within stability limit).

Fig. 6 shows the block diagram of the proposed ripple elimination method. The reference active current with 2nd-order harmonic is generated from the voltage controller. The 2nd-order harmonic current can be extracted by using the PR controller. It is possible to compensate the harmonic by subtracting this from the reference active current.

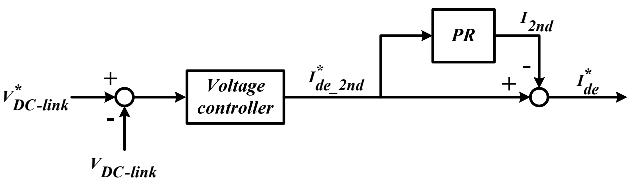

Fig. 6. Block diagram of proposed ripple elimination method.

5. Simulations

Fig. 7 shows the reference DC-link voltage and the DC-link voltage with the 2nd-order harmonic. The reference active current subjected to the influence of the 2nd-order harmonic causes the distortion into the output current.

Fig. 8 shows the reference active current with 2nd-order harmonic. The active current follows the reference active current. Therefore, the active current follows not the DC component of reference active current but also the 2nd-order harmonic.

Fig. 9 shows 2nd-order harmonic obtained by using the PR controller. It is possible to pick out the 2nd-order harmonic from the reference active current. This harmonic can be used to compensate the reference active current as a kind of feed forward component.

Fig. 10 shows the reference active current after 2nd-order harmonic compensation. It is possible to compensate the reference active current by simply subtracting the 2nd-order harmonic from the reference active current with 2nd-order harmonic.

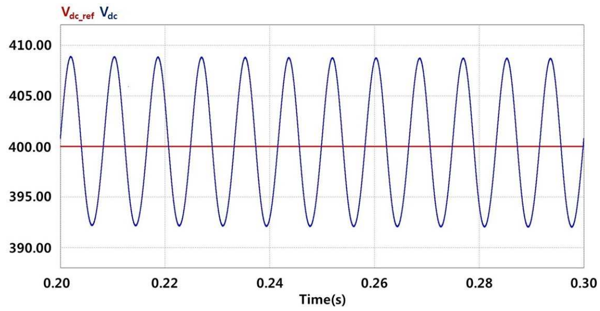

Fig. 7. Reference DC-link voltage and the DC-link voltage with 2nd-order harmonic.

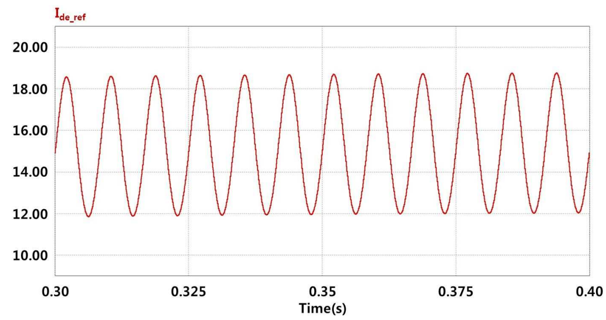

Fig. 8. Reference active current with 2nd-order harmonic.

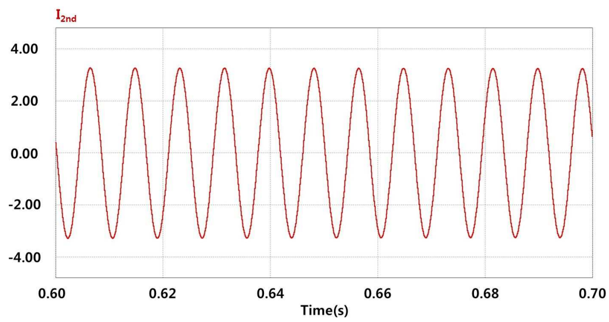

Fig. 9. 2nd-order harmonic obtained by using the PR controller.

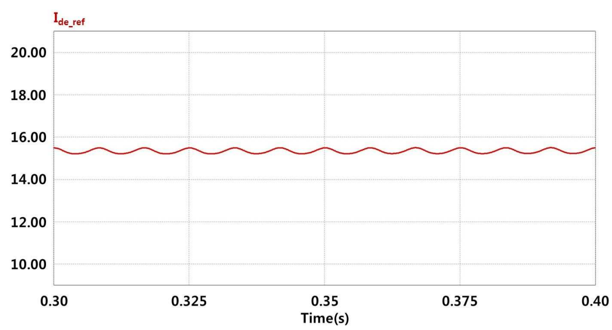

Fig. 10. Reference active current after the 2nd-order harmonic compensation.

Fig. 11 and 12 show the FFT form of the reference active current before and after the 2^{nd}-order harmonic compensation. It can be seen that the harmonic have been compensated.

Fig. 13 and 14 show the output current before and after the harmonic compensation. The 2^{nd}-order harmonic in the active current is transformed to 1^{st} and 3^{rd}-order harmonic through the frame transformation for SPWM. The 1^{st} and 3^{rd}-order harmonic makes the output current to be distorted. Therefore, it is possible to compensate the output current by reducing the 2^{nd}-order harmonic in the reference active current. It can be seen that the output current close to a sinusoidal wave, which has no 3^{rd}-order harmonic.

Fig. 15 and 16 show the FFT form of the output current before and after the 2^{nd}-order harmonic compensation. It can be seen that the 3^{rd}-order harmonic have been reduced.

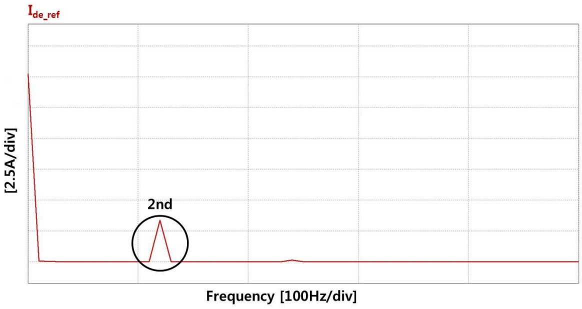

Fig. 11. FFT form of the reference active current before the 2^{nd}-order harmonic compensation.

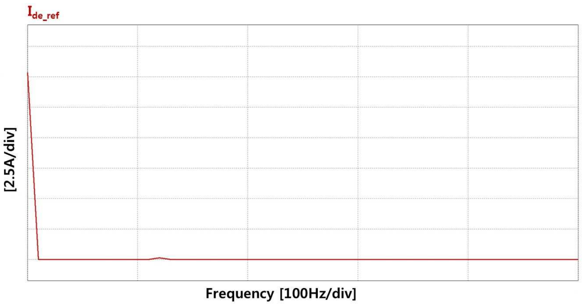

Fig. 12. FFT form of the reference active current after the 2^{nd}-order harmonic compensation.

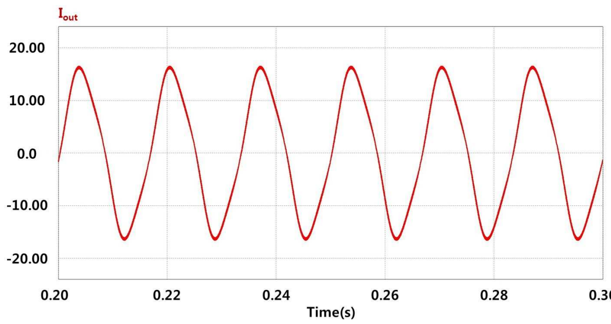

Fig. 13. Output current before the 2^{nd}-order harmonic compensation.

The grid frequency is not always constant as 60Hz. Thus, the calculated value which is the 2^{nd}-order harmonic of DC-link voltage is not correct. In addition, the BSF

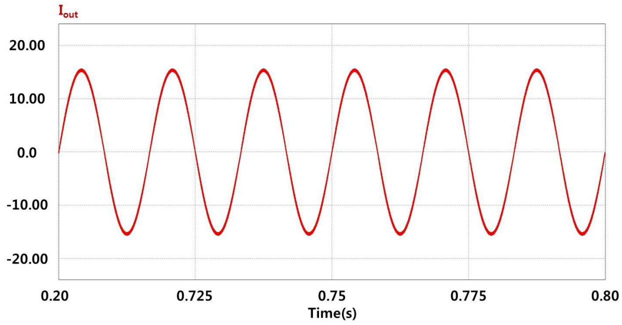

Fig. 14. Output current after the 2^{nd}-order harmonic compensation.

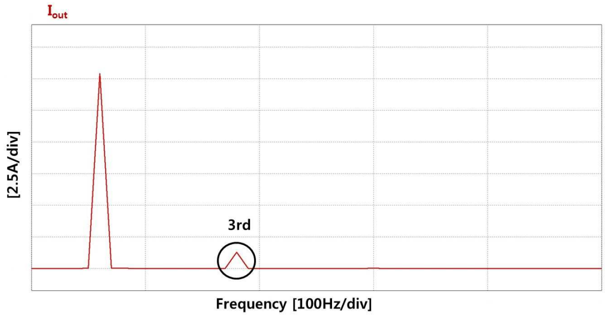

Fig. 15. FFT form of the output current before the 2^{nd}-order harmonic compensation.

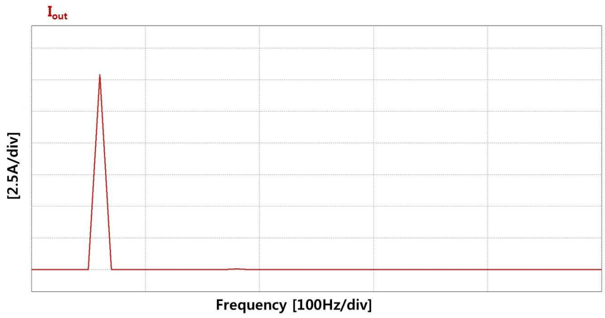

Fig. 16. FFT form of the output current after the 2^{nd}-order harmonic compensation.

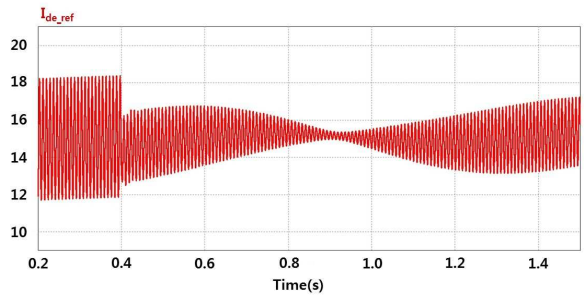

Fig. 17. Reference active current when the conventional method is applied.

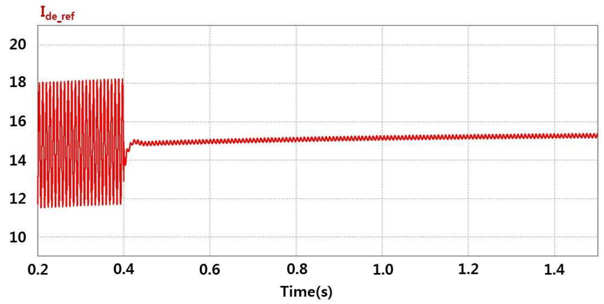

Fig. 18. Reference active current when the proposed method is applied.

designed to reduce the 120Hz harmonic cannot compensate appropriately the actual occurred 2nd-order harmonic. However, the proposed method using the PR controller does not make the error which made by the calculation and is not affected by the variable grid frequency because the bandwidth of PR controller can be controlled. Fig. 17 shows the reference active current when the conventional method is applied. Fig. 18 shows the reference active current when proposed method is applied. The grid frequency is 59.5Hz. The compensation is done at 0.4 second. When using the conventional method, the 2nd-order harmonic ripple of the reference active current is not reduced but resonant. On the other hand, it can be seen that the 2nd-order harmonic ripple of the reference active current is reduced and stable when using the proposed method. It can be confirmed the effectiveness of the proposed method under the condition that grid frequency is 59.5Hz.

6. The Experimental Results

Fig. 19 shows the DC-link voltage wave form with the 2nd-order harmonic and its FFT form. A DC-link voltage of a single-phase wind power system has the 2nd-order harmonic, inevitably. This harmonic have a harmful effect on the reference active current and the output current.

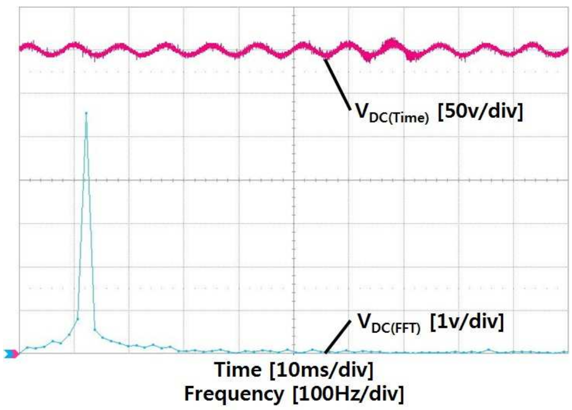

Fig. 19. DC-link voltage with the 2nd-order harmonic.

Fig. 20 and 21 represent the reference active current before and after the 2nd-order harmonic compensation. The 2nd-order harmonic has been reduced by 82.23%. The 2nd-order harmonic compensation makes the output current to be compensated.

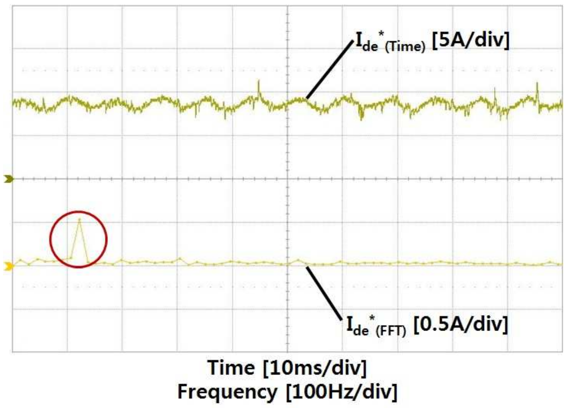

Fig. 20. Reference active current before the 2nd-order harmonic compensation.

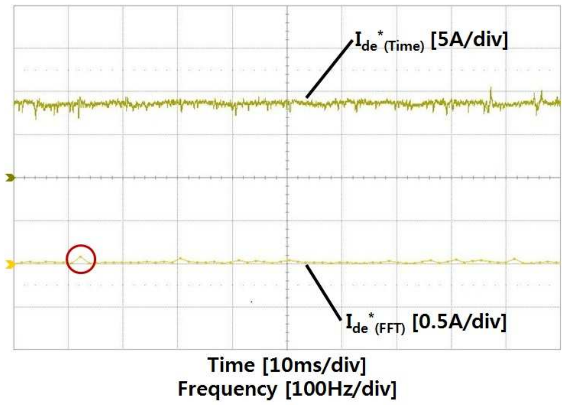

Fig. 21. Reference active current after the 2nd-order harmonic compensation.

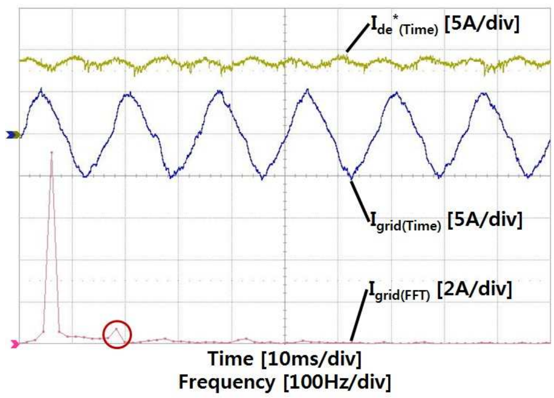

Fig. 22. Reference active current, output current, FFT form of the output current before the 2nd-order harmonic compensation.

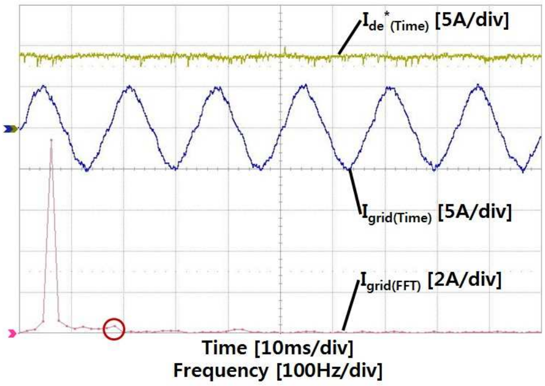

Fig. 23. Reference active current, output current, FFT form of the output current after the 2nd-order harmonic compensation.

Fig. 22 and 23 displays the reference active current, the output current, and the FFT of the output current before and after the 2nd-order harmonic compensation. It can be seen that the ripple of the reference active current is reduced by compensating the 2nd-order harmonic. The FFT of the output current is compensated by increasing the 1st-order harmonic and eliminating the 3rd-order harmonic. The 1st-order harmonic is increased by 2.22%. The 3rd-order harmonic is reduced by 81.13%. The harmonic compensation makes the output current to close a sinusoidal wave.

7. Conclusion

This paper has proposed a 2nd-order harmonic compensation method using the PR controller for the wind power system. The PR controller can be used as a feed-forward compensator because the PR controller can compensate the harmonic selectively. The 2nd-order harmonic in the DC-link voltage has a bad impact on the output current in the end. The conventional method can compensate the 2nd-order harmonic as the PR controller when the complex calculation is correct. However, the proposed method does not require the complex computation and additional filter. The simulation and experimental results confirm the feasibility and effectiveness of the proposed method.

Acknowledgements

This work was supported by a National Research Foundation of Korea (NRF) grant funded by the Korea government (MEST) (No.20120002247)

References

[1] M. Liserre, R. Teodorescu, and F. Blaabjerg, "Stability of Photovoltaic and Wind Turbine Grid-Connected Inverters for a Large Set of Grid Impedance Values", *IEEE Transactions on Power Electronics*, Vol. 21, No. 1, pp. 263-272, Jan. 2006.

[2] D. K. Choi and K. B. Lee, "Stability Improvement of Distributed Power Generation Systems with an LCL-Filter using Gain Scheduling based on Grid Impedance Estimations", *Journal of Power Electronics*, Vol. 11, No. 4, pp. 599-605, Jul. 2011.

[3] K. W. Park and K. B. Lee, "Hardware Simulator Development for a 3-Parallel Grid-Connected PMSG Wind Power System", *Journal of Power Electronics*, Vol. 10, No. 5, pp. 555-562, Sept. 2010.

[4] P. Rodriguez, A. Timbus, R. Teodorescu, M. Liserre, and F. Blaabjerg, "Reactive Power Control for Improving Wind Turbine System Behavior Under Grid Faults", *IEEE Transactions on Power Electronics*, Vol. 24, No. 7, pp. 1798-1801, Jul. 2009.

[5] Z. Chen, Y. Hu, and F. Blaabjerg "Stability improvement of induction generator-based wind turbine systems", *in Proceedings of the IEEE IET Renewable Power Generation*, Vol. 1, No. 1, pp. 81-93, Mar. 2007.

[6] A. M. Sharaf, and A. A. A. Elgammal "Power Efficient PID Controller of Wind Driven Induction Generation Single-Phase Induction Motors for Electric Energy Saving Applicaions", *in Proceedings of the IEEE Electric Power and Energy Conferences*, pp. 1-6, Aug. 2010.

[7] K. Fujinami, K. Takahashi, K. Kondo, and Y. Sato, "A Restarting Method of an Induction Motor Speed-Sensorless Vector Control System for a Small-Sized Wind Turbine Power Generator System", *in Proceedings of the IEEE ICEMS2009*, pp. 1-5, Nov. 2009.

[8] S. H. Lee, T. P. An, and H. J. Cha, "Mitigation of Low Frequency AC Ripple in Single-Phase Photovoltaic Power Conditioning Systems", *Journal of Power Electronics*, Vol. 10, No. 3, pp. 328-333. May. 2010.

[9] J. G. Lee, and J. W. Choi, "The Elimination Method of Ripple Voltage for a Single Grid-Connected PV System", *in Proceedings of the Power Electronics Annual Conference*, pp. 406-407, Jul. 2011.

[10] Y. K. Kang, H. G. Jung, K. B. Lee, D. C. Lee, and J. M. Kim, "A Simple Estimation Scheme of the Initial Rotor Position and Inductances for an Effective MTPA-Operaion in a Wind-Power System using an IPMSM", *Journal of Power Electronics,* Vol. 10, No. 4, pp. 396-404, jul. 2010.

[11] R. Bharanikumar, M. Prabha Maheswari, and S. Palanichamy, "Boost Chopper Circuit for Low Power Wind Turbine Driven PM Synchronous Generator", *in Proceedings of the IEEE ICIAS2007*, pp. 859-863, Nov. 2007.

[12] P. C. Tan, P. C. Loh, and D. G. Holmes, "High performance harmonic extraction algorithm for a 25kV traction power quality conditioner", *in Pro-*

ceedings of the IEE Electric Power Applications, Vol. 151, No. 5, pp. 505-512, Sept. 2004.

[13] D. N. Zmood and D. G. Holmes, "Stationary Frame Current Regulation of PWM Inverters with Zero Steady-State Error", *IEEE Transactions on Power Electronics*, Vol. 18, No. 3, pp. 814-822, May. 2003.

[14] G. Xiaoqiang, Z. Qinglin, and W. Weiyang, "A Single-Phase Grid-Connected Inverter System With Zero Steady-State Error", *in Proceedings of the IEEE Power Electronics and Motion Control Conference*, Vol. 1, pp. 1-5, Aug. 2006.

[15] J. H. Lee, H. G. Jung, and K. B. Lee, "Performance Improvement of Grid-Connected Inverter Systems under Unbalanced and Distorted Grid Voltage by Using a PR Controller", *Journal of Electrical Engineering & Technology*, Vol. 7, No. 6, pp. 918-925, Nov. 2012.

[16] R. Teodorescu, F. Blaabjerg, M. Liserre, and P. C. Loh, "Proportional-resonant controllers and filters for grid-connected voltage-source converters", *in Proceedings of the IEE Electric Power Applications*, Vol. 153, No. 5, pp. 750-762, Sept. 2006.

Hae-Gwang Jeong He was born in Jeonju, Korea, in 1982. He received the B.S. degree in Electrical Engineering from Chonbuk National University, Jeonju, Korea, in 2008. He is currently working toward the M.S. degree at Ajou University. His research interests are power conversion and electric ma-chine drives.

Jong-Hyun Lee He was born in Jeonju, Korea, in 1985. He received the B.S. degree in Electrical and Computer Engineering from Ajou University, Suwon, Korea, in 2011. He is currently working toward the M.S. degree at Ajou University, Suwon, Korea. His research interests are power conversion and electric machine drives.

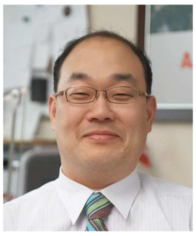

Kyo-Beum Lee He was born in Seoul, Korea, in 1972. He received the B.S. and M.S. degrees in Electrical and Electronic Engineering from the Ajou University, Korea, in 1997 and 1999, respectively. He received the Ph.D. degree in electrical engineering from the Korea University, Korea in 2003. From 2003 to 2006, he was with the Institute of Energy Technology, Aalborg University, Aalborg, Denmark. From 2006 to 2007, he was with the Division of Electronics and Information Engineering, Chonbuk National University, Jeonju, Korea. In 2007 he joined the Division of Electrical and Computer Engineering, Ajou University, Suwon, Korea. He is an associate editor of the IEEE Transactions on Power Electronics, Industrial Electronics, and the Journal of Power Electronics. His research interests include electric machine drives, renewable power generations, and electric vehicles.